Supporting Information

Bimetallic aluminum complexes with cyclic β-ketiminato ligands: cooperative effect improves capability in polymerization of lactide and ε-caprolactone

Hai-Chao Huang,[a] Bin Wang,[a] Yan-Ping Zhang [a] and Yue-Sheng Li[*a,b]

[a] Tianjin Key Lab Composite & Functional Materials, School of Materials Science and Engineering, Tianjin University, Tianjin 300072, China

[b] Collaborative Innovation Center of Chemical Science and Engineering (Tianjin), Tianjin 300072, China

[*]Corresponding Author, E-mail: ysli@tju.edu.cn

Table S1. Crystal data and structure refinements of complexes **4a-c**

	4a	4b	4c
Empirical formula	$C_{28} H_{34} Al_2 N_2 O_2$	$C_{32} H_{40} Al_2 N_2 O_2$	$C_{31} H_{40} Al_2 N_2 O_2$
Formula weight	484.53	538.62	526.61
Crystal system	Monoclinic	Monoclinic	Triclinic
Space group	P2(1)/c	P2(1)/c	P-1
Temperature(K)	113(2)	113(2)	113(2)
Wavelength(A)	0.71073	0.71075	0.71073
a(Å)	10.649(2)	10.1875(7)	7.4541(8)
b(Å)	10.0527(18)	23.8487(16)	12.2711(13)
c(Å)	12.321(2)	12.0803(8)	15.7103(15)
α (°)	90.00	90.00	77.640(6)
β (°)	98.931(4)	96.1673(16)	81.252(6)
γ (°)	90.00	90.00	80.078(6)
V(Å3),Z	1303.0(4), 2	2918.0(3), 4	1372.8(2), 2
Densitycalcd(Mg/m^3)	1.235	1.226	1.274
Absorptioncoefficient(mm^{-1})	0.139	0.131	0.137
F(000)	516	1152	564
Crystal size/mm	0.20 x 0.18 x 0.12	0.100 x 0.080 x 0.080	0.20 x 0.18 x 0.12
θ range for data (°)	3.11 to 27.50	1.710 to 28.723	3.06 to 27.55
Reflections collected	16257	39454	17806
Independent reflections	2981	7499	6207
	R(int) = 0.0181	R(int) = 0.0213	R(int) = 0.0226
Data/restraints/parameters	2981/0/156	7499/0/343	6207/0/334
Goodness-of-fit on F^2	1.048	1.045	1.038
Final R indices [I>2σ (I)]: R1, wR2	R1 = 0.0292	R1 = 0.0334	R1 = 0.0328
	wR2 = 0.0852	wR2 = 0.0929	wR2 = 0.0937
Largest diff. Peak and hole (e Å^{-3})	0.365 and -0.235	0.416 and -0.330	0.385 and -0.365

Table S2 Selected bond distances (Å) and angles (°) for complexes **4a-c**

	4a	4b	4c
	Bond distances		
Al(1)-O(1)	1.8004(9)	1.7990(9)	1.7988(9)
Al(1)-N(1)	1.9359(10)	1.9448(10)	1.9497(11)
Al(1)-C(13)	1.9605(12)	1.9539(13)	1.9565(13)
Al(1)-C(14)	1.9611(13)	1.9609(12)	1.9628(13)
O(1)-C(1)	1.3119(13)	1.3097(12)	1.3151(14)
N(1)-C(11)	1.3080(14)	1.3171(14)	1.3071(15)
N(1)-C(12)	1.4696(13)	1.4761(12)	1.4785(14)
	Bond angles		
O(1)-Al(1)-N(1)	94.48(4)	94.82(4)	93.91(4)
O(1)-Al(1)-C(13)	114.99(5)	110.16(5)	111.89(5)
N(1)-Al(1)-C(13)	108.88(5)	111.22(5)	109.77(5)
O(1)-Al(1)-C(14)	112.21(5)	108.36(5)	106.87(5)
N(1)-Al(1)-C(14)	110.42(5)	113.69(5)	112.49(5)
C(13)-Al(1)-C(14)	114.06(5)	116.39(6)	119.04(6)
C(1)-O(1)-Al(1)	129.43(7)	128.14(7)	121.21(7)
C(11)-N(1)-Al(1)	122.87(7)	120.13(7)	117.88(8)
C(12)-N(1)-Al(1)	120.56(7)	123.66(7)	123.91(8)
	The distances between Al(1) and Al(2)		
Al(1)- Al(2)	6.617	5.965	7.770

Table S3 Ring-opening polymerization of *L*-LA and ε-CL by **4a-c**/*i*PrOH system [a]

Run	Complex	Mono.	[Al]/[OH]/[M]	*time* (min)	Conv. (%)	TOF[b] (h^{-1})	$M_{n,\text{theo}}$[c,d] ($\times 10^4$)	M_n[f] ($\times 10^4$)	M_w/M_n[f]
1	**4a**	ε-CL	1:1:100	10	97	582	1.11	1.54	1.17
2	**4b**	ε-CL	1:1:100	10	64	384	0.73	0.87	1.14
3	**M1**	ε-CL	1:1:100	10	43	258	0.49	0.52	1.14
4	**4c**	ε-CL	1:0:100	7	--	--	--	--	--
5	**M2**	ε-CL	1:1:100	7	84	720	0.96	1.00	1.12
6	**4c**	ε-CL	1:1:100	3	83	1660	0.95	0.97	1.19
7	**4c**	ε-CL	1:2:100	3	89	1780	0.51	0.53	1.21
8	**4c**	ε-CL	1:4:100	3	85	1700	0.24	0.29	1.27
9	**4c**	ε-CL	1:2:200	6	89	890	1.02	1.09	1.21
10	**4c**	ε-CL	1:2:400	12	91	455	2.08	2.36	1.24
11	**4c**	ε-CL	1:2:600	15	93	372	3.19	3.32	1.22
12	**4c**	ε-CL	1:2:800	20	90	270	4.11	4.46	1.25
13	**4c**	ε-CL	1:2:1000	30	94	188	5.36	5.53	1.23
14	**M2**	ε-CL	1:2:200	6	69	73	0.79	0.89	1.21
15	**M2**	ε-CL	1:2:400	12	71	355	1.62	2.01	1.22
16	**M2**	ε-CL	1:2:600	16	74	296	2.54	2.95	1.26
17	**M2**	ε-CL	1:2:800	20	65	195	2.97	3.39	1.24
18	**M2**	ε-CL	1:2:1000	30	63	126	3.59	3.86	1.25
19	**4a**	*L*-LA	1:1:100	240	36	9	0.52	0.58	1.08
20	**4b**	*L*-LA	1:1:100	240	trace	--	--	--	--
21	**4c**	*L*-LA	1:1:100	10	20	120	0.29	0.27	1.08
22	**4c**	*L*-LA	1:1:100	15	42	168	0.60	0.72	1.07
23	**4c**	*L*-LA	1:1:100	30	74	148	1.07	1.34	1.12
24	**4c**	*L*-LA	1:1:100	45	89	119	1.28	1.70	1.14
25	**4c**	*L*-LA	1:1:100	60	97	97	1.40	1.89	1.22
26	**4c**	*rac*-LA[g]	1:1:100	60	95	95	1.37	1.64	1.23
27	**M2**	*L*-LA	1:0:100	90	--	--	--	--	--
28	**M2**	*L*-LA	1:1:100	90	79	53	1.14	1.02	1.18

[a] 25 μmol of Al complex in 2 mL toluene, and polymerization at 80 °C; [b] Non-optimized turnover frequency calculated over the whole reaction time; [c] Calculated $M_{n,\text{theo}}=[\varepsilon\text{-CL}]_0/[\text{OH}]\times\text{conv.}(\varepsilon\text{-CL})\times114.14+M_{i\text{PrOH}}$; [d] Calculated $M_{n,\text{theo}}=[L\text{-LA}]_0/[\text{OH}]\times\text{conv.}(L\text{-LA})\times144.13+M_{i\text{PrOH}}$; [f] Experimental M_n values were determined by GPC analysis in THF using polystyrene standards and corrected by the equation: $M_n=0.58\times M_{n(\text{GPC})}$ for PLA, and $M_n=0.56\times M_{n(\text{GPC})}$ for PCL. [g] $P_m=0.33$.

Table S4 Synthesis of PLA-*b*-PCL copolymer by **4c**/*i*PrOH system [a]

Entry	Complex	Time[b]	$M_{n,GPC}$ [c] (10^{-4})	M_n [d] (10^{-4})	M_w/M_n
PLA-*b*-PCL[e]	4c	1.5h(LA)+1h(CL)	4.0	2.12	1.34

[a] Reaction conditions: 25 μmol complex in toluene, *i*PrOH 1.0 equiv. to Al, monomer 5.0 mmol, 80 °C; [b] After LA reaction for 1.5 h, CL was added and reacted for the prescribed time; [c] GPC data determined by SEC in THF relative to polystyrene standards; [d] GPC data determined by SEC in THF relative to polystyrene standards corrected by the Mark–Houwink correction factor ($M_n=M_{n,SEC} \times 0.56 \times PCL\% + M_{n,SEC} \times 0.58 \times PLLA\%$); [e] the first block PLA with $M_{n,GPC}=1.83 \times 10^4$, $M_w/M_n=1.21$, conversion > 99%

Table S5. Experimental T_g of the CL/LA copolymers as a function of the mole fraction of ε-CL unit

Entry	Time (h)	CL in copolymer [b] (%)	T_g (°C)
1	0.5	14.5	43
2	1	21.8	35
3	2	45.1	2.4
4	3	50.0	-2.6

[a] Reaction conditions: 25 μmol of Al catalyst in 2 mL of toluene, *i*PrOH/[Al] = 2.0, [CL]/[LA]/[Al]=100:100:1, copolymerization at 80 °C; [b] CL in copolymer measured by ^{1}H NMR.

Table S6. Calculate reactivity ratios for *L*-LA and ε-CL in Poly(LA-*grad*-CL) copolymers [a]

Entry	Conv. (%)	X [b]	Y [c]	G [d]	F [e]
1	3.1	0.43	3.15	0.29	0.059
2	5.4	1.0	6.67	2.11	0.58
3	5.4	2.3	14.3	4.71	1.39
4	4.7	9.0	33.3	8.73	2.43

[a] Reaction conditions: 25 μmol of Al catalyst in 2 ml of toluene, [*i*PrOH]/[Al] = 2.0, 80 °C; The reactivity ratios were calculated using the nonlinear least squares (NLLS) method, the monomer composition in the obtained oligomer was examined at a low conversion (≤10%).
[b] X = M_{LA}/M_{CL}, M_{LA} and M_{CL} were defined as moles of monomer in the copolymerization reaction system;
[c] Y was defined as the mole ratio of two kinds of monomer;
[d] G = X (Y−1)/Y;
[e] F = X^2/Y^3.

Table S7. Copolymerization of ε-CL and L-LA with different monomer ratio by **4a**/^{i}PrOH system [a]

Run	LA:CL :Al:OH (mol:mol)	Conversion (%)	M_n[b] /10^{-4}	M_w/M_n[b]	L_{CL}[c]	L_{LA}[c]	CL (mol %)[d]
1	400:100:1:1	trace	--	--	--	--	--
2	200:100:1:1	29	0.84	1.31	5.25	27.6	24.7
3	100:100:1:1	41	1.12	1.39	3.36	20.8	21.2
4	100:200:1:1	46	1.38	1.37	4.61	29.1	17.8
5	100:400:1:1	19	0.69	1.41	--	--	--

[a] Reaction conditions: 25 μmol of Al catalyst and copolymerization at 80 °C for 8 h; [b] Determined by GPC in THF using polystyrene as standard; [c] Average sequences length of the caproyl unit and lactidyl unit was determined by ^{13}C NMR; [d] Monomer conversion was determined by ^{1}H NMR. [d] CL in the copolymer (mol %)
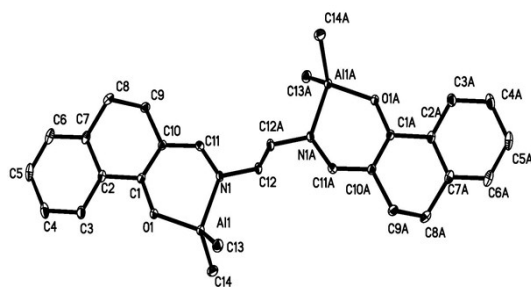
Fig. S1. Molecular structure of complex **4a** with thermal ellipsoids at the 30% probability level. Hydrogen atoms are omitted for clarity.
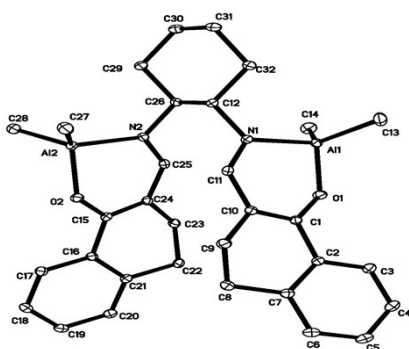
Fig. S2. Molecular structure of complex **4b** with thermal ellipsoids at the 30% probability level. Hydrogen atoms are omitted for clarity.
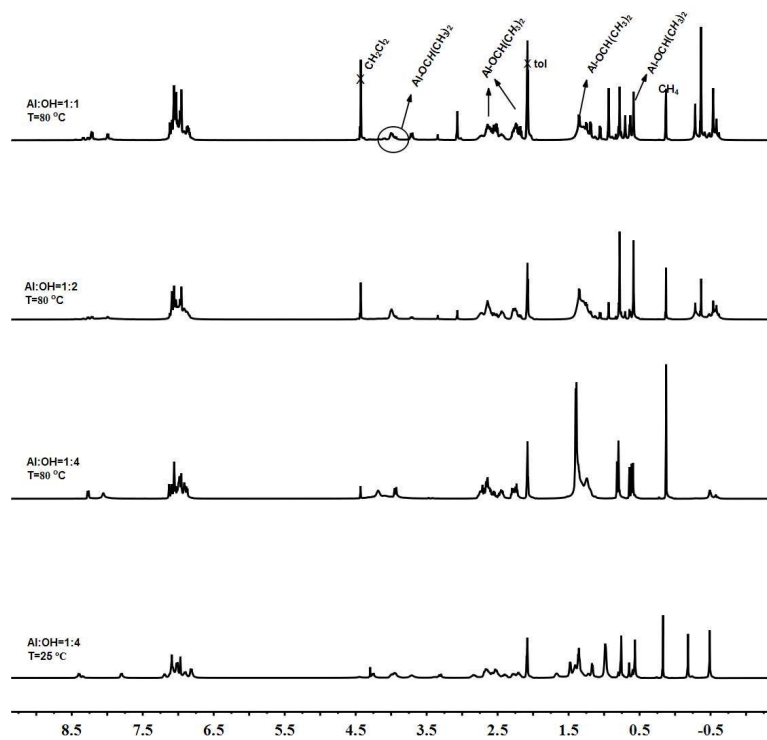
Fig. S3. ^{1}H NMR spectrum of binuclear aluminum complexes **4c** in the presence of [i]PrOH (toluene-d_8, 400 MHz)
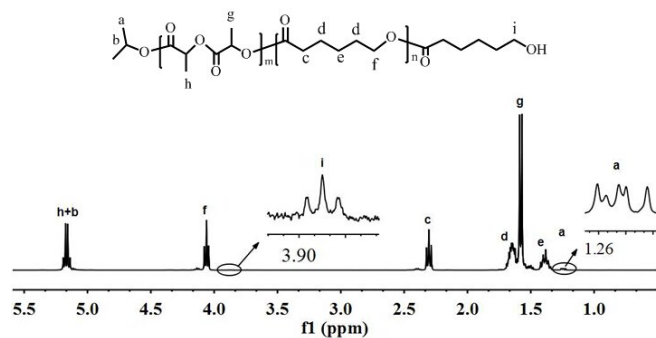
Fig. S4. Methyne proton of the hydroxyl end group of the PLA-*b*-PCL copolymer (CDCl$_3$, 25 °C).
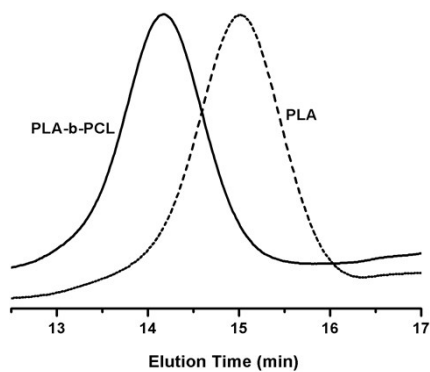
Fig.S5. GPC profiles of PLA and PLA-*b*-PCL obtained by the **4c**/*i*PrOH system (in THF at 25 °C).
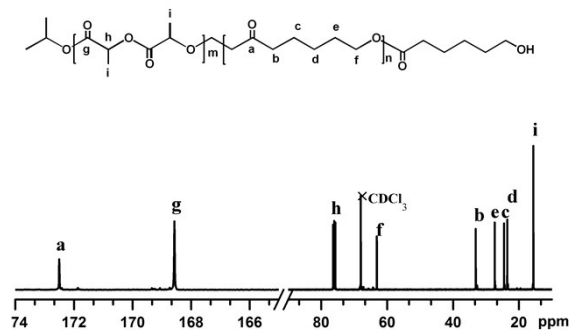
Fig. S6. ^{13}C NMR spectrum of PLA-*b*-PCL synthesized by **4c**/*i*PrOH system (CDCl$_3$, 25 °C).
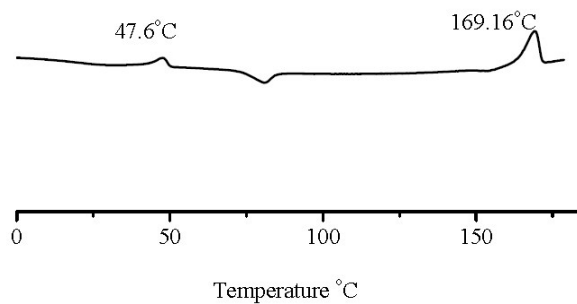
Fig. S7. DSC curve of PLA-*b*-PCL prepared by **4c**/*i*PrOH system.
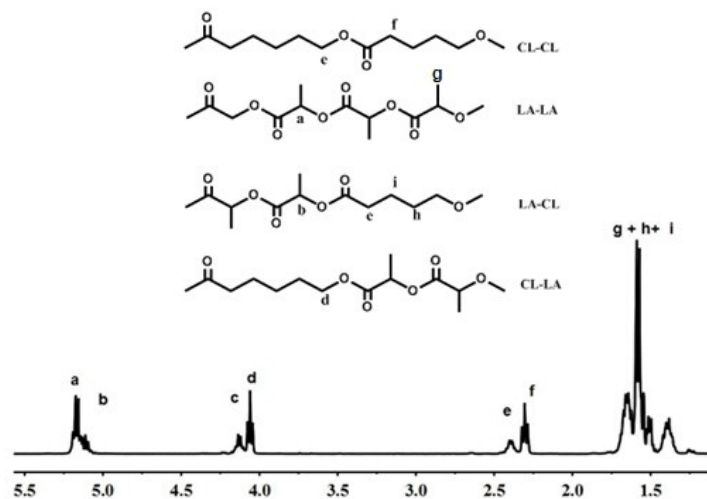
Fig. S8. ^{1}H NMR spectrum of poly(LA-*grad*-CL) copolymer (run 2, Table 3) (CDCl$_3$, 25 ^{o}C).
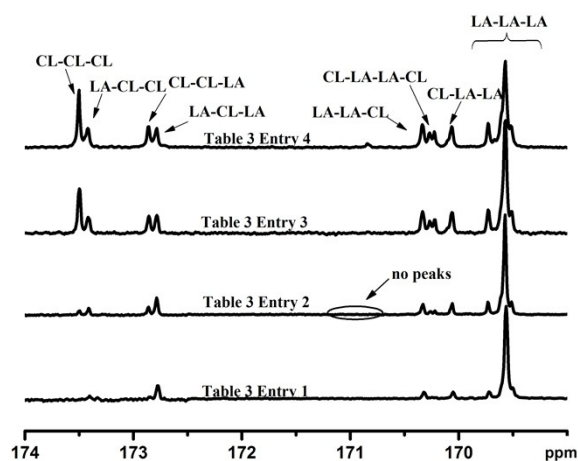
Fig. S9. ^{13}C NMR spectra (CDCl$_3$, 25 ^{o}C) of the copolymers obtained at different conversion.
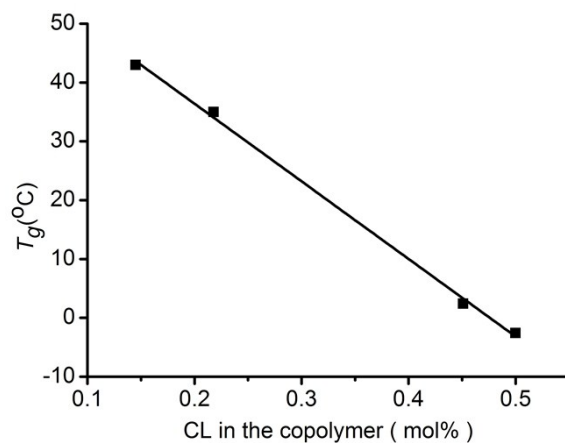
Fig. S10. Experimental T_g of the CL/LA copolymers as a function of the mole fraction of ε-CL unit.
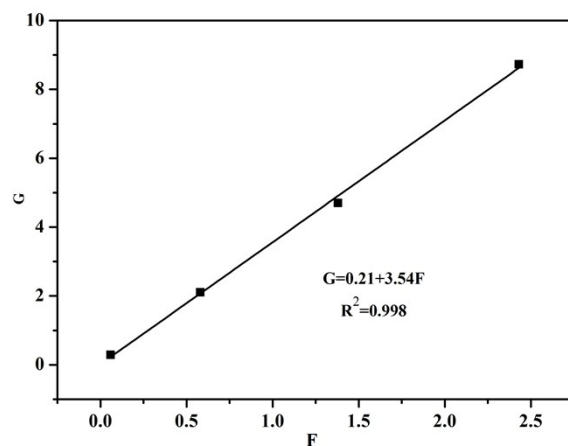
Fig. S11. G-F plot for Poly(LA-*grad*-CL) copolymers by **4c**/^{i}PrOH system.
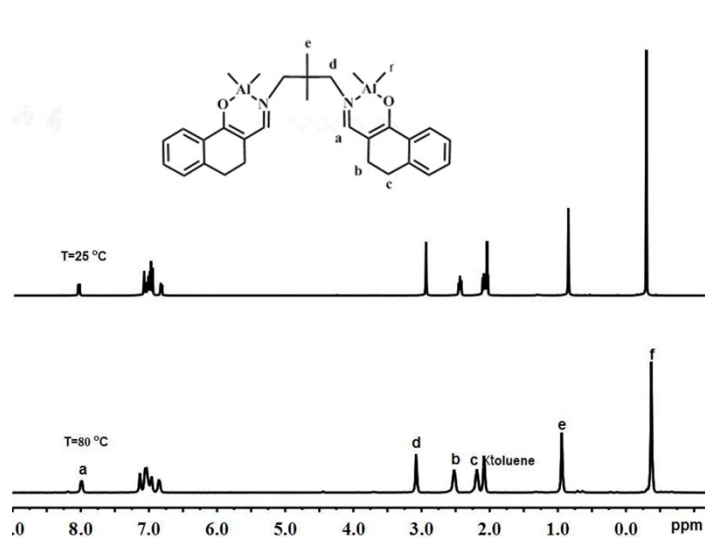
Fig. S12. ^{1}H NMR spectrum of binuclear aluminum complexes **4c** (toluene-d$_8$,400 MHz)
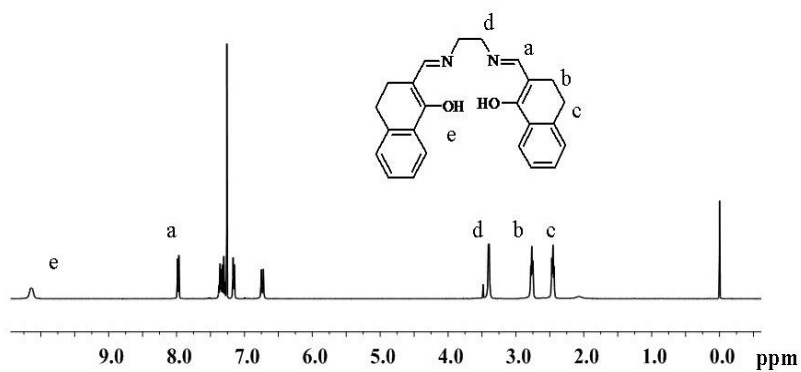
Fig. S13. ^{1}H NMR spectrum of β-ketiminato ligand **3a** (CDCl$_3$, 25 ℃).
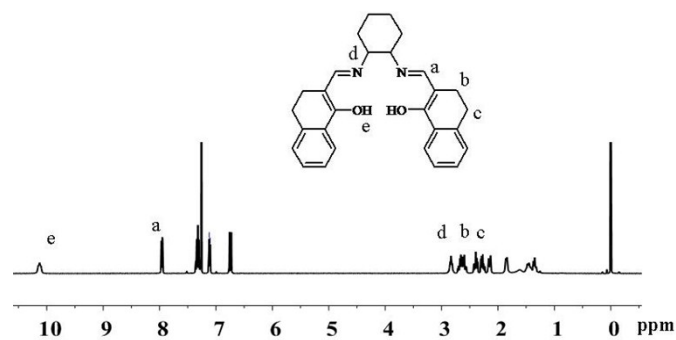
Fig. S14. ^{1}H NMR spectrum of β-ketiminato ligand **3b** (CDCl$_3$, 25 °C).
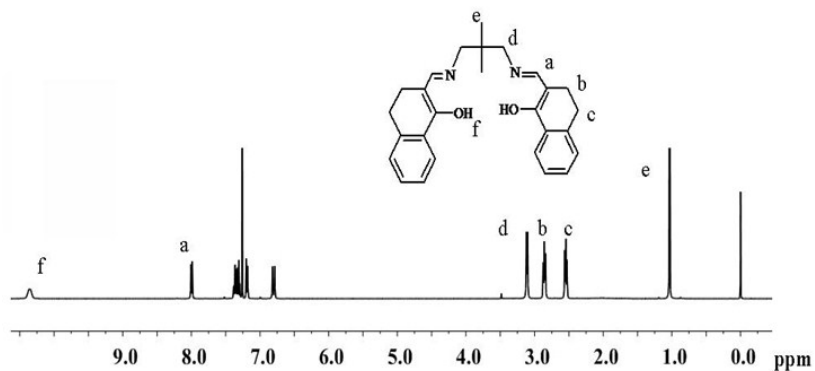
Fig. S15. ^{1}H NMR spectrum of β-ketiminato ligand **3c** (CDCl$_3$, 25 °C).
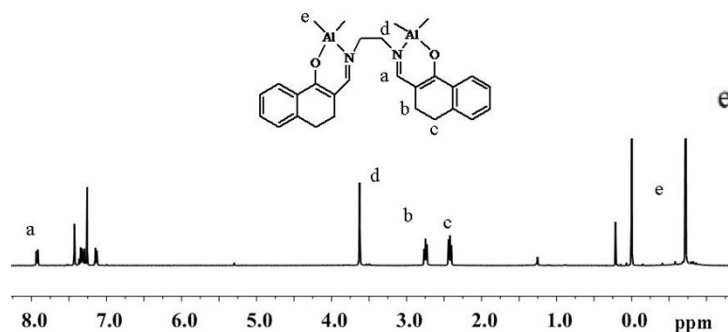
Fig. S16. ^{1}H NMR spectrum of binuclear aluminum complexes **4a** (CDCl$_3$, 25 °C).
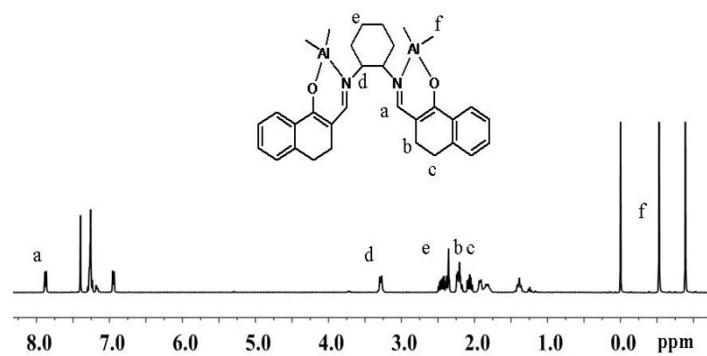
**Fig. S17.** ^{1}H NMR spectrum of binuclear aluminum complexes **4b** (CDCl$_3$, 25 °C).
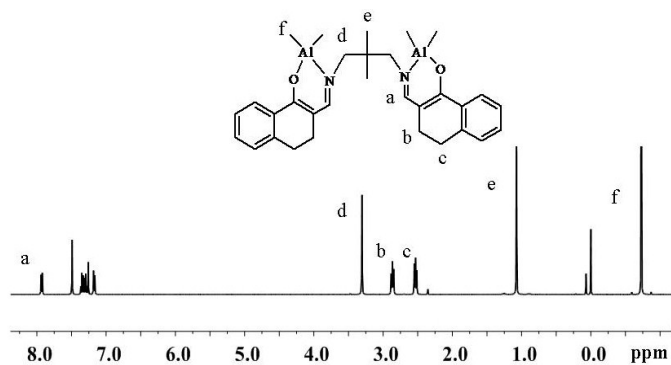
**Fig. S18.** ^{1}H NMR spectrum of binuclear aluminum complexes **4c** (CDCl$_3$, 25 °C).
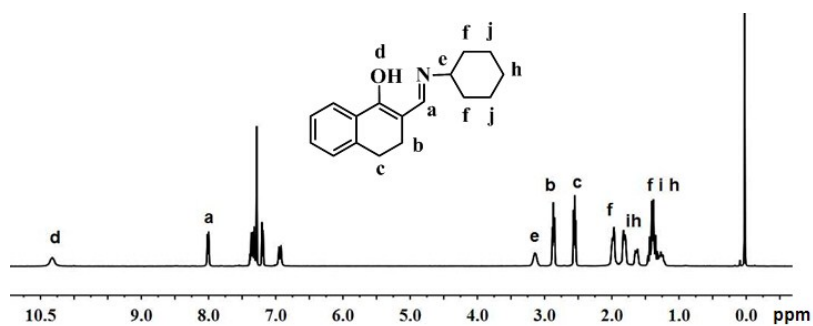
Fig. S19. ^{1}H NMR spectrum of β-ketiminato ligand for **M1** (CDCl$_3$, 25 °C).
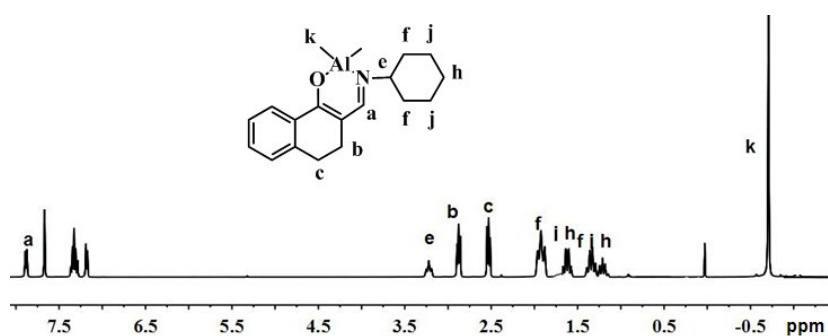

Fig. S20. ^{1}H NMR spectrum of mononuclear aluminum complex **M1** (CDCl$_3$, 25 °C).
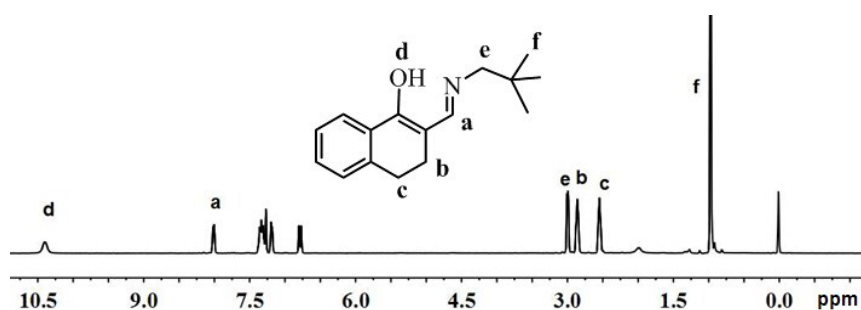

Fig. S21. ^{1}H NMR spectrum of mononuclear aluminum complex for **M2** (CDCl$_3$, 25 °C).
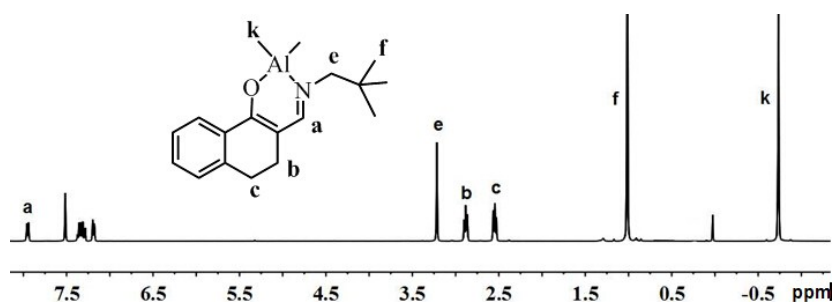
Fig. S22. ^{1}H NMR spectrum of mononuclear aluminum complex **M2** (CDCl$_3$, 25°C).

Synthesis of aluminum complexes M1 and M2

Into a stirred solution of **C$_6$H$_{11}$N=CHC$_4$H$_4$(C$_6$H$_4$)OH** (2.0 mmol) in toluene (10 mL), AlMe$_3$ (1 M hexane solution, 2.1 mL) was added drop-wise over 10 min. After stirred for 8 h the solution was concentrated and cooled to -20 °C, yellow solid was isolated by filter and recrystallized from mixture of toluene/hexane and afforded **[C$_6$H$_{11}$N=CHC$_4$H$_4$(C$_6$H$_4$)O] Al(CH$_3$)$_2$ (M1)** Yield:92%.^{1}H NMR (400 MHz, CDCl$_3$) 7.88 (d, 1H, N = C-*H*), 7.67 (s, 1H, Ar-*H*), 7.33 (m, 2H, Ar-*H*), 7.18 (d, 1H, Ar-*H*), 3.22 (dd, 1H, C*H*-(CH$_2$)$_2$), 2.95–2.77 (m, 2H,-C*H$_2$*-), 2.62–2.47 (m, 2H, -C*H$_2$*-), 1.92 (t, 4H,-CH-C*H$_2$*), 1.80–1.02 (m, 6H), -0.71 (s, Al-C*H$_3$*, 6H). ^{13}C NMR (100 MHz, CDCl$_3$):166.33, 139.73, 133.29, 130.76, 127.15, 126.69, 125.93, 104.37, 67.35, 31.08, 28.69, 25.94, 25.56, 25.15, 24.5, -8.45.

Synthesis for **[C(CH$_3$)$_3$CHN=CHC$_4$H$_4$(C$_6$H$_4$)O] Al(CH$_3$)$_2$ (M2)** was performed according to the same procedure as that of **M1** Yield:88% .^{1}H NMR (400 MHz, CDCl$_3$) 7.95 (d, 1H, N = C-*H*), 7.51 (s, 1H, Ar-*H*), 7.42–7.25 (m, 2H, Ar-*H*), 7.19 (d, 1H, Ar-*H*), 3.22 (s, 2H -C*H$_2$*-CH), 2.95–2.78 (m, 2H, -C*H$_2$*-), 2.66–2.46 (m, 2H, -C*H$_2$*-), 1.01 (s, 9H, C*H$_3$*), -0.73 (d, 6H, Al-C*H$_3$*). ^{13}C NMR (100 MHz, CDCl$_3$):166.46, 139.45, 133.18, 130.87, 127.26, 126.75, 125.97, 106.16, 67.57, 33.97, 28.51, 25.84, 25.39, 25.17, -8.65.